J Ther Eng, Vol. 10, No. 3, pp. 697−709, May, 2024

Journal of Thermal Engineering
Web page info: https://jten.yildiz.edu.tr
DOI: 10.14744/thermal.0000814

Research Article

# Numerical simulation of aerodynamic performance of the wing with edge of attack and sinusoidal escape

**Mustafa A. MOHAMMED[1], Marwah Ali HUSAIN[2,*]**

*[1]Department of Mechanical Engineering, College of Engineering, Al-Nahrain University, Baghdad, 64074, Iraq*
*[2]Department of Refrigeration and Air Conditioning Engineering Techniques, Alsalam University College, Baghdad, 10001, Iraq*

## ARTICLE INFO

*Article history*
Received: 06 July 2022
Accepted: 14 February 2023

**Keywords:**
Aerodynamic Performance; Drag Coefficient; Edge of Attack and Sinusoidal Escape; Lifting Coefficient; Turbulence; Wings

## ABSTRACT

Wings are one of the engineering components that play a vital role in the aerospace industry. Therefore, increasing the performance of the wings can improve the overall performance of the airplanes. One way to increase wing performance is to use sinusoidal curvature at the attack edge and wing escape, which delays the phenomenon of fatigue and improves aerodynamic performance at high attack angles. This study is to provide a better understanding of the aerodynamic characteristics of a finite NACA0012 wing with the performance of a wing with different types of wings with sinusoidal attack edge, sinusoidal escape edge, and compared them with simple wing. ANSYS FLUENT method has been used to simulate the wings. In addition to, the TRANSITION SST-4EQ method has also been used to solve the governing equations. The aerodynamic performance of a wing with the performance of different types of wings with sinusoidal attack edge, sinusoidal escape edge, and simple wing with NACA0012 cross section are investigated in Reynolds numbers of 5000, 15000 and 60,000 numerically. The kinetic energy distribution of turbulence on the wing body in these Reynolds numbers has been investigated. The amount of coefficients for and after different wings in Reynolds number 15000 with changing angle has been analyzed. In unstable conditions, compressibility and non-viscosity have been compared. According to the present study, it was observed that the maximum pressure around the wing is sinusoidal and the wing with a combined design is higher than the simple wing. The drag is related to the wing with the combined design, although this geometry has the highest value of drag in the article with other types of wings.

**Cite this article as:** Mohammed MA, Husain MA. Numerical simulation of aerodynamic performance of the wing with edge of attack and sinusoidal escape. J Ther Eng 2024;10(3):697−709.

## INTRODUCTION

Throughout the past century, researches and developments have been conducted on wings, which contributes to a constructive role in designing wind turbines, ship rudder, missiles and aviation industries. NACA0012 is a well-known airfoil that is utilized in academic researches as well as industrial applications such as Mini-Unmanned Aerial Vehicle (MUAV) [1]. Today, due to the importance of wings and their widespread use in the aircraft industry, many researchers

***Corresponding author.**
*E-mail address: marwah.a.husain@alsalam.edu.iq

*This paper was recommended for publication in revised form by Regional Editor Erman Aslan*

Published by Yıldız Technical University Press, İstanbul, Turkey

have decided to increase the aerodynamic performance of wings and optimize them by providing various solutions [2]. One of the ways to increase wing performance is to be inspired by nature. The humpback whale is one of the marine animals that, despite having large bodies, has a very high speed and agility when swimming. Therefore, some researchers by studying the wings of this animal and using its geometry in the wings tried to increase the performance of the wings. Among the basic researches in the field of using the geometry of humpback whales in the wings, we can mention the research of Fish et al. [3] which was done in 2008. In this study, they divided a humpback whale into different parts and studied its geometry. According to the results, it was observed that the presence of a sinusoidal attack edge on the wing of this creature has increased the movement control by this animal and also increased the amount of lifting force for this creature. With increasing attention to the sinusoidal wing, Huang et al. [4] in one study evaluated the performance of the sinusoidal wing in the wind tunnel. They also placed a simple wing in similar conditions to allow a comparison between the two types of wings. In these experiments, it was observed that creating a sinusoidal attack edge on a wing can increase the fatigue angle by about 40%. Based on the lifting rate obtained in the experiments, although the sinusoidal wing showed a lower lifting rate than the simple wing, but after exhaustion, it had a much higher lifting force than it. Research has also been done by Post et al. [5] on the wing with a sinusoidal edge and its effect on the type of flow. In this study, it was observed that the sinusoidal attack edge causes the separation of the rotation in the direction of the flow width in the high angle of attack. In this type of geometry, two non-coaxial vortices are formed when the current strikes the indentation edge of the attack, which are transmitted along the flow. Accordingly, the current accelerates in the direction of the ridge of the attack edge due to the interaction with the vortex pair, which prevents the local separation of the downstream boundary layer from the sinusoidal edge of the attack and delays the exhaustion line to the escape edge. In another study by Mehraban et al. [6], the use of a sinusoidal edge using different wavelengths and amplitudes on the aerodynamic performance of a wing was investigated. In addition to, simple and sinusoidal lift and drag coefficients were compared. In this study, it was also observed that before the occurrence of fatigue, the coefficient of elevation in the simple wing is higher than the sinusoidal wing. However, after exhaustion, the elevation coefficient in the wing with a sinusoidal attack edge is 50% higher than the elevation coefficient in the simple wing. It was also observed that after the occurrence of exhaustion, the amount of drag coefficient in a simple wing does not change much with the angle, while in the sinus wing, after the occurrence of fatigue, the drag coefficient increases sharply and is very sensitive to angle. In this study, it was observed that sine wave size plays a very small role in the aerodynamic performance of the wing. Wang et al. [7] also performed studies on the sinus fin function of NACA 021-63. In this study, various characteristics of the fin, including the amount of lift, drag and moment of a fin with a sinusoidal attack edge, were tested and measured. In the designed geometry, the wavelength in the direction of the fin opening was in the range of 25 to 50% of the chord length and the changes of the sine advancing edge in the yield of 2.5 to 12% of the chord length were considered. Based on the obtained data, it was observed that the amount of drag coefficient did not change with increasing the angle of attack from 0 to 3 degrees, but with increasing it from 3 to 15 degrees, the rate of drag coefficient increased. In addition to, by passing the approximate angle of 15 degrees and reaching the angle of attack of 21 degrees, the amount of drag coefficient has been fixed again, but after passing the angle of 21 degrees, the drag coefficient has decreased sharply. In this experiment, it was observed that the bar coefficient is always ascending with increasing the angle of attack up to 21 degrees, but when it reaches the stall area (21 degrees), its rate decreases sharply. Guo et al. [8] Torsion in the wing and its effect on aerodynamic performance According to this study, the creation of torsion in the wing with a sinusoidal attack edge delays fatigue and thus prevents a drop in the coefficient. MacPhee et al. [9] in an experimental study examining the aerodynamic performance of a simple wing with a sinusoidal curvature by placing the wing in a wind tunnel found that curvature reduced the drag coefficient by 28% and increased the lift coefficient. It has been observed that by increasing the Reynolds number from 77 thousand to 174 thousand, the coefficient of elevation has increased and the exhaustion angle has also increased by 33%. The performance of an inverted fin with a smooth and sinusoidal attack edge has also been investigated by Butt et. al [10]. To study this type of fin, the geometry is placed in a water tunnel at a Reynolds number of 14,000 and at torsion angles of 0 to 20 degrees. Based on the results obtained in this study, the current separation in the fin with a smooth edge occurred rapidly and the effects of increasing the torsion angle from 0 to 20 degrees on the effects of separation gradually appeared, but this phenomenon in the fin with a sinusoidal attack edge is greatly reduced. Found and delayed. Based on this study, it was observed that the use of sinusoidal edge increases the flight time of the aircraft without using engine power. Ahmed et al. [11] numerically examined the behavior of lift and drag coefficients of NACA0012 at 0° to 50° angle of attack using a k – ω shear stress transport (SST) turbulence model. The number of nodes was increased to reach a cell number of 120000 to have a satisfactory mesh size and accurate results. The results show that for a Mach number of 0.2 and 10° angle of attack, the lift and drag coefficients are 0.019 and 0.001, respectively. On the other hand, by increasing the angle of attack to 50°, the lift coefficient drops to 0.015, while the drag coefficient increases to 0.006. In another study, Zhang et al. [12] numerically studied the flow field of NACA0012 at 0° to 180° using C-type grid with 360 cells, H-type grid with 200 cells and O-type grid with 320 cells. The Mach number and Reynold's number were set to 0.15 and 0.5 × 106, respectively. The simulation was performed for angle of attack ranging

from 10° to 70° utilizing Spalart-Allmaras, standard k – ε, RNG k – ε, as well as SST k – ωturbulent model. The simulations were conducted for 0° to 180° angle of attack on the NACA0012 utilizing Spalart-Allmaras turbulence model. Comparison of the numerical for different grid topologies shows that C-type grid has the best fit to the experimental results while coefficients obtained from the H-type and O-type grid show a great scatter at angle of attack. Hence the C-type grid was found to be a more reliable grid type, compared to O-type and H-type. Windi et al. [13] conducted a 2-D numerical analysis on the flow separation around NACA0012 at different angles of attack ranging from 0° to 20° using the k – ε turbulent model. The results from the analysis show that increasing the angle of attack results in significant separation of the flow. The flow is observed to be laminar below 10° angle of attack. From 0° to 10° angle of attack there is no separation and lift coefficient increases while the drag coefficient is nearly constant. Increments after 10° result in increase of adverse pressure gradient on the upper surface, which causes turbulence. It was also found that the lift coefficient increases until 12° angle of attack without significant change in drag coefficient and the separation happens at the tail of the airfoil. The separation continues growing until a critical angle of attack (stall angle) of 15°, in which the flow is fully separated from the upper surface of airfoil and the lift coefficient increases slowly while the drag coefficient increases dramatically. A numerical study was conducted by Laouira et al. [14] to investigated the heat transfer phenomena inside a horizontal channel with an open trapezoidal enclosure subjected to a heat source of different lengths. The heat source was considered as a local heating element of varying length, which was embedded at the bottom wall of the enclosure and maintained at a constant temperature. The air flow enters the channel horizontally at a constant cold temperature and a fixed velocity. The other walls of the enclosure and the channel were kept thermally insulated. The flow was assumed laminar, incompressible, and two-dimensional, whereas the fluid is considered Newtonian. The results were presented in the form of the contours of velocity, isotherms, and Nusselt numbers profiles for various values of the dimensionless heat source lengths ($0.16 \leq \varepsilon \leq 1$). while, both Prandtl and Reynolds numbers were kept constant at (Pr = 0.71) and (Re = 100), respectively. The results indicated that the distribution of the isotherms depends significantly on the length of the heat source. In addition to, it was noted that both the local and the average Nusselt numbers increase as the local heat source length increases. In another study by Hassan et al. [15] deliberated the flow and heat transfer of a shear thinning fluid over a non-linear stretching sheet has variable thickness. All rheological aspects at low to high shear rates are accounted theoretical by using generalized Carreau model of viscosity. The results of skin friction coefficient and Nusselt number are obtained under effects of these parameters. It is found that Nusselt number is significantly decreased when stretching is increased by velocity index parameter. The use of sinusoidal edging edge in the study of Miklosovic and Murray [16] on wing performance with NACA0012 cross section has been investigated. The effect of using sinusoidal edges with different wavelengths was also investigated. According to this study, increasing the sine wave edge wavelength increases the force density. In addition to, based on the distribution of oscillating energy, this criterion is much higher at the wing escape edge than at the attack edge. In fact, the closer we get to the edge of the attack, the lower the oscillating energy. In another study by Pendar et al. [17], the characteristics of cavitation current around a wing with a sinusoidal attack edge were investigated. The results of cavitation current around the wing with a sinusoidal attack edge are compared with the outputs of the simulation of a wing with a smooth attack edge, the amplitude of sinusoidal geometry oscillation was considered as 5 and 25% of the chord length and its wavelength was considered as 25 and 50% of the chord geometry length. The development of the rate of separation of slow flow bubbles in the suction part of the wing with the sinusoidal attack edge has led to the prevention of flow separation. In addition to, the geometry with the sine attack edge has erratic fluctuations in aerodynamic forces at the frequency of vortices compared to the smooth attack edge. Due to the very good performance of sinusoidal edge of the wing attack with a simple edge of attack has caused the control of the current on the wing and has had a great effect on controlling the flow fatigue.

Previous studies have examined the aerodynamics of NACA0012 airfoils and different types of wings with different angles of attack. However, the available data for finite wing aerodynamic characteristics at low Reynold's numbers are limited. The aim of this study is to provide a better understanding of the aerodynamic characteristics of a finite NACA0012 wing with the performance of a wing with different types of wings with sinusoidal attack edge, sinusoidal escape edge, and compared them with simple wing. ANSYS FLUENT method has been used to simulate the wings. In addition to, the TRANSITION SST-4EQ method has also been used to solve the governing equations. The pressure and velocity distribution around the wings at variable angles of attack in Reynold's number of 5000, 15000 and 60,000 is presented. The kinetic energy distribution of turbulence on the wing body in these Reynolds numbers has also been investigated. In addition, the amount of coefficients for and after different wings in Reynolds number 15000 with changing angle has been analyzed. The findings of the study enable aeronautical industries to have a detailed understating of the flow behavior at such low-speed flight regime.

## NUMERICAL METHODOLOGY

In the present problem, simple wing geometry, wing with sine attack edge, wing with sine escape edge and wing with combined design are designed simultaneously using NACA0012 cross section shape. In this study, considering that the base airfoil for all wings is NACA0012, it is possible

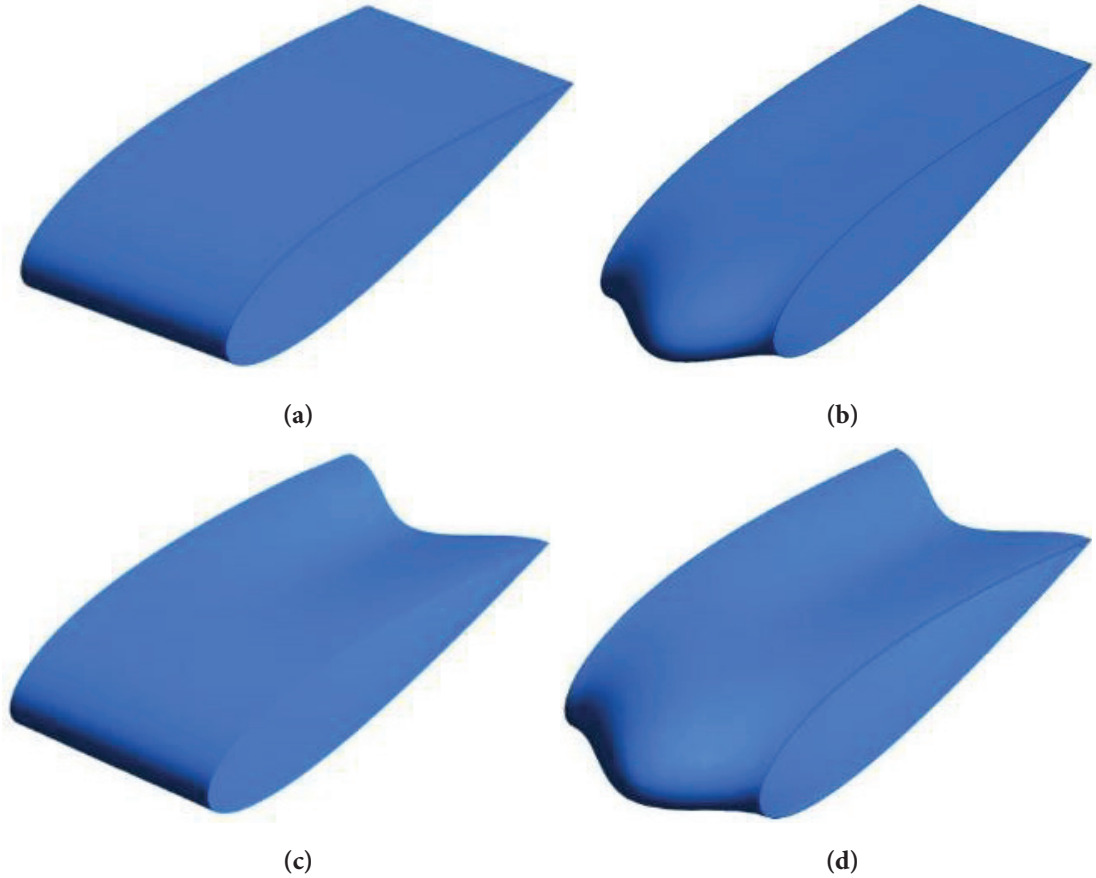


**Figure 1.** Designed wing geometry (a) simple wing (b) sine attack edge wing (c) sinusoidal escape edge wing and (d) combined wing.

to compare the output results. To produce a sinusoidal edge on the wing with a chord length of 1 m and a sinusoidal attacking edge with a wavelength profile of 30 mm and an amplitude of 8 mm is considered. The geometries produced are shown in Figure 1.

In the present study, the designed geometry has been solved in a three-dimensional way using the finite element method using ANSYS Fluent commercial software. The governing equations of flow physics are as follows:

Conservation of energy:

$$\frac{\partial}{\partial t}(\rho E) + \nabla.\left(\vec{V}(\rho E + \rho)\right) = -\nabla.\left(\sum_j h_j J_j\right) + S_h \quad (1a)$$

Continuity equation:

$$\frac{\partial \rho}{\partial t} + \frac{\partial(\rho u)}{\partial x} + \frac{\partial(\rho v)}{\partial y} + \frac{\partial(\rho w)}{\partial z} = 0 \quad (1b)$$

For incompressible

$$\frac{\partial u}{\partial x} + \frac{\partial v}{\partial y} + \frac{\partial w}{\partial z} = 0 \quad (1c)$$

Momentum equation:

$$\begin{aligned} \rho\frac{Du}{Dt} &= \frac{\partial(-P+\tau_{xx})}{\partial x} + \frac{\tau_{yx}}{\partial y} + \frac{\tau_{zx}}{\partial z} + S_1\rho\frac{Dv}{Dt} \\ &= \frac{\tau_{xy}}{\partial x} + \frac{\partial(-P+\tau_{yy})}{\partial y} + \frac{\tau_{zy}}{\partial z} + S_2\rho\frac{Dw}{Dt} \\ &= \frac{\tau_{xz}}{\partial x} + \frac{\tau_{yz}}{\partial y} + \frac{\partial(-P+\tau_{zz})}{\partial z} + S_3 \end{aligned} \quad (2)$$

In these equations ρ, P are the symbols of density, pressure and *u*, *v* and *w* are the components of flow velocity and S1, S2 and S3 are the source expressions. It should be noted that in order to solve these equations in ANSYS Fluent commercial software, the unstable modeling method is due to the type of flow physics and the formation of primary vortex pairs, which due to the overlap of vortex clockwise and counterclockwise vortices causes the formation of secondary vortices. The solver used for the equations is also selected according to the pressure-base flow velocity. In order to pair the equations of pressure and velocity, the simple method with the second-order approach has been used. In addition to, in order to solve the flow in Fluent software, the TRANSITION-SST-4eq transfer model has been used.

## Numerical Simulation

### Wing geometry and fluid domain

Numerical simulations have recently developed a good reputation in engineering researches. One of the applicable numerical methods is the computational fluid dynamics (CFD) [18]. Computer software has been utilized CFD in the research methodology to expedite the research process and to reduce the cost of prototypes and experiments. In order to achieve reliable results through simulation process, it is important to apply the right meshing method and boundary conditions. The numerical simulations in this paper are conducted using ANSYS FLUENT. In order to simulate the wing and evaluate its performance due to movement in the air, the part of the wing that had symmetry was selected and placed within a computational volume. In this numerical geometry, due to the high computational cost and symmetry of the wing geometry as well as the lack of differences in the output results, only one part of the geometry is designed. The space around the wing geometry is also considered to be large to prevent the effects of the current around the wing on the walls of the computational range. Figure 2 shows the range intended for numerical solution.

### Numerical setup

To solve the problem, the intended fluid is in the space around the air wing so that it enters from the front plate which is defined as "inlet velocity" and exits from the end plate which is defined as "outlet pressure". In addition to, the wing plates are selected as "walls" provided they do not slip. The side walls are also selected as "periodic" according to the symmetry of the geometry, which is also shown in Figure 2. In addition to, the assumptions on which the simulation is based are as follows:

- Using the turbulent model TRANSITION SST-4EQ to solve turbulence modeling due to the higher accuracy of this equation than using the slow flow solution method [20].
- Existence of non-slip condition on the wing.
- Simulation of a part of wing geometry due to geometry symmetry.
- Ignoring the roughness of the wing surface.

It should be noted that the sine ratio for the edge of the wing attack is as follows:

$$x_{LE} = A \sin\left(\frac{2n\pi z}{s}\right), \quad 0 \le z \le s \tag{3}$$

In the above equation, z is the position relative to the wing aperture and A is the sine wavelength.

$$x_1 = \begin{cases} \left[x + 0.5x_{LE}\left(1 + \cos\cos\left(\frac{\pi x}{0.3c}\right)\right)\right] & 0 \le x \le 0.3c \\ 1 & x \ge 0.3c \end{cases} \tag{4}$$

In the above equation, $x$ is the base profile of the wing and $x_1$ is the cross-sectional profile. The derivative of the above equation is also used to rotate the radius of the edge of the attack, as follows:

$$\frac{dx_1}{dx} = \begin{cases} \left[1 - \frac{0.5x_{LE}\pi}{0.3c} \sin\sin\left(\frac{\pi x}{0.3c}\right)\right] & 0 \le x \le 0.3c \\ 0 & x \ge 0.3c \end{cases} \tag{5}$$

### Mesh

A fine mesh is one of the requirements to achieve accurate simulation results. The C-type grid topology is utilized in this research as it is found to be the efficient meshing method for wing geometry [19]. A fine mesh (Figure 3) is achieved and implemented by defining edge sizing and inflation layers on the edge of the wing geometry and sweeping the achieved mesh along the wing span.

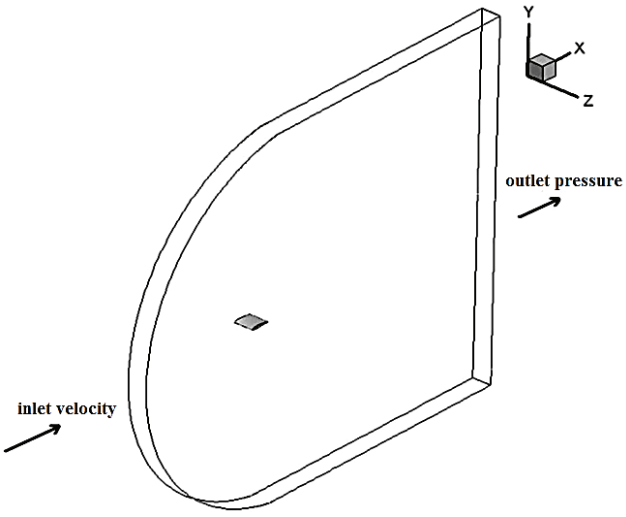


**Figure 2.** Fluid domain around the wing.

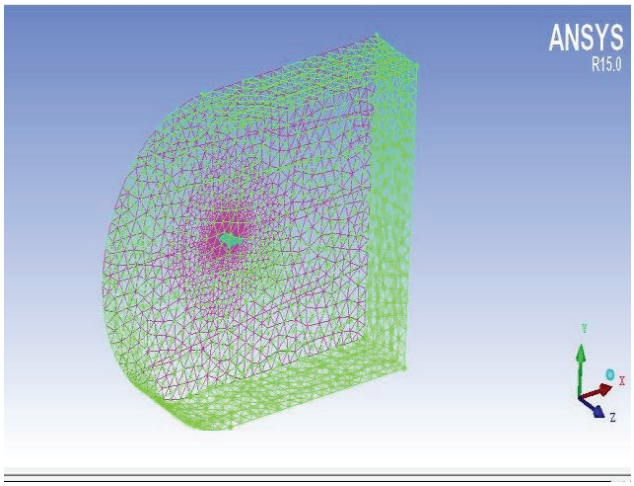


**Figure 3.** Mesh of the fluid domain.

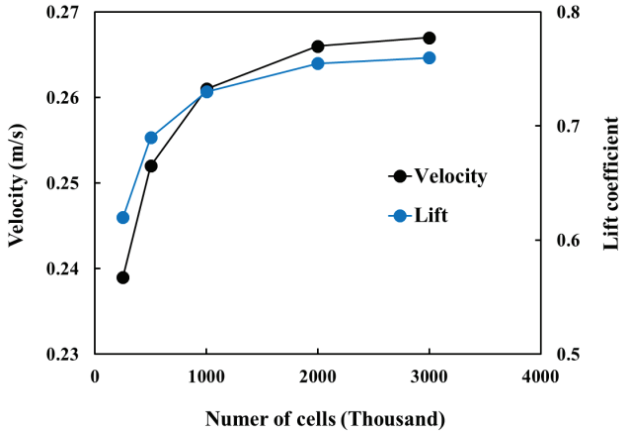


**Figure 4.** Maximum flow velocity on the side of the wing with a combined design and coefficient of elevation of this type of wing in different networks.

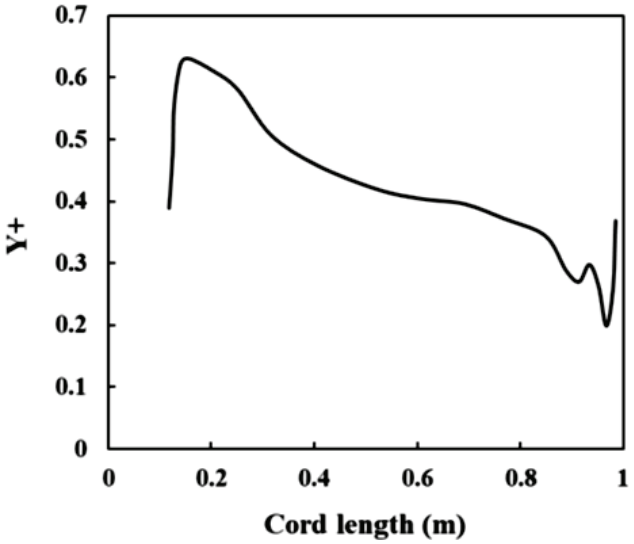


**Figure 5.** Y + distribution on the central line of the airfoil in the network with 2000 thousand cells.

In numerical solution problems, due to the limited computational cost, creating a network with minimum computational cost and maximum accuracy is essential. Therefore, in this study, in order to reduce the computational cost and at the same time provide appropriate accuracy in the answers, several networks with 250, 500, 1000, 2000 and 4000 thousand cells have been produced and analyzed. To evaluate the results in different networks, wing geometry with volatile edge and sinusoidal attack were used simultaneously, and the maximum flow velocity and the coefficient of wing production in terms of cell number were examined.

In Figure 4, the rate of change of the studied parameters (coefficient of erection and flow velocity) is observed in terms of the number of cells in the network. Based on the obtained results, the difference between the results in the network with 2000 and 4000 thousand cells is about 0.3% and the percentage of accepted error in the article of Hansen et al. [20] is below 0.35%, so according to the results. The obtained grid is used with 2000 thousand cells, and due to the importance of Y+ in numerical simulations, the value of this quantity has been tried to be in the standard range selected is displayed as shown in Figure 5.

## RESULTS AND DISCUSSION

### Validation of Results

In order to validate the obtained numerical results, the results obtained from the simulated lift and post-wing coefficient have been compared with the results obtained in the study of Hansen et al. [20]. Based on the results, in

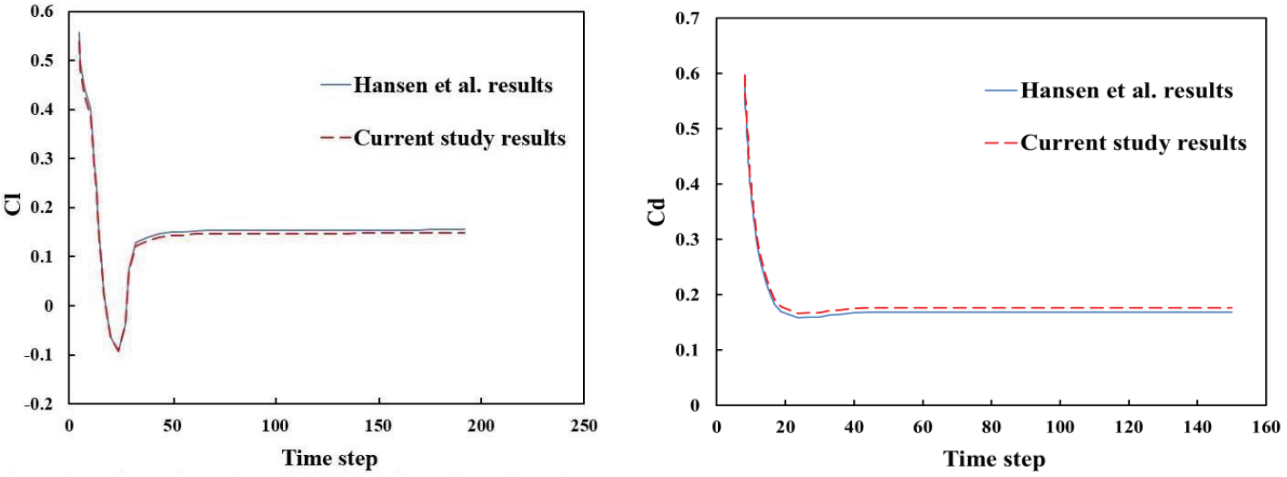


**Figure 6.** Comparison of the present numerical solution and the results of the study of Hansen et al. [20] (a) coefficient CI (b) coefficient of drag Cd.

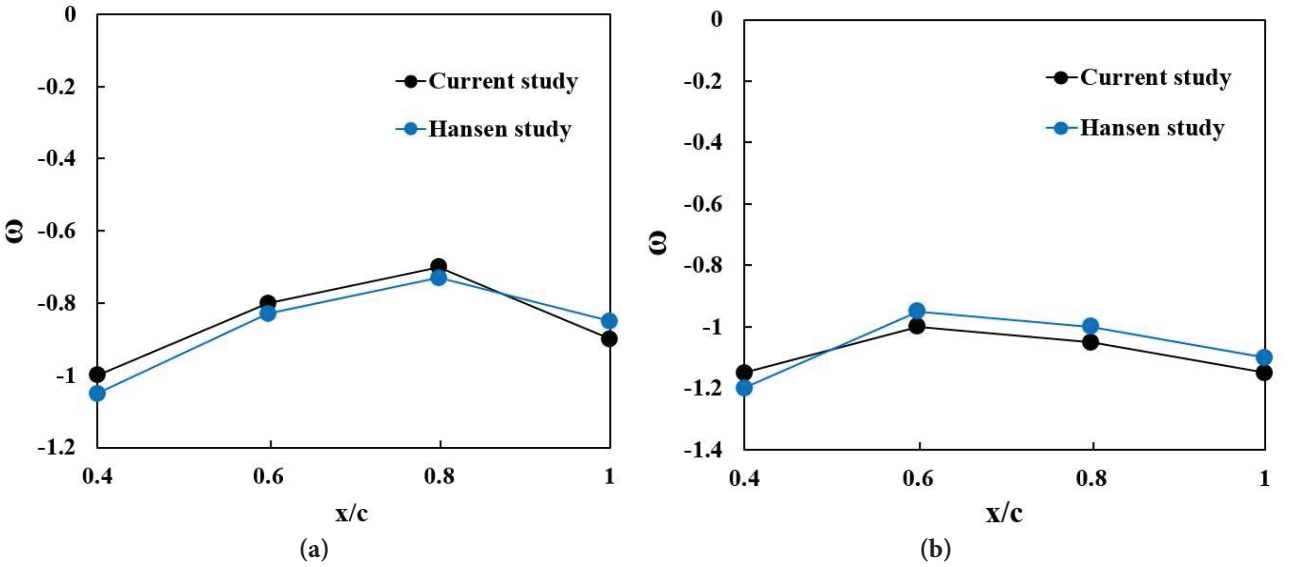


**Figure 7.** Comparison of the rotation rate in the central section of the airfoil in the present study and the results of Hansen et al. [20] in the angle of attack (a) 5 degrees and (b) 10 degrees.

both studies, the coefficient of elevation was very high at first, but with the passage of time and the stability of the problem, the coefficient of elevation decreases and then tends to a constant value. This behavior is also observed in the simulated post-wing coefficient. Based on the results obtained in Reynolds number 2230, the difference between the results of the present study and the study of Hansen et al. [20] is about 2.1%. In addition to, the error rate between the results for the drag coefficient is about 2.8%. Figure 6 (a) and (b) show the up and down wing coefficients at a 10° angle of attack, respectively.

In addition, in order to be more sure of the output results, the rotation rate in the central section of the airfoil obtained in the present study and the study of Hansen et al. [20] have been compared with each other. Figure 7 (a) and (b) show the rotation angles at 5° and 10° and Reynolds 2330, respectively. The degree is 4.59 and 4.73 percent, respectively, which indicates the appropriate accuracy of the present study.

**Aerodynamic Characteristics of the Wing with Edge of Attack and Sinusoidal Escape**

This section first presents the results of the simulation of the wing with a sinusoidal attack edge. Based on the results obtained from the pressure and velocity distribution around the wing with a sinusoidal attack edge, the maximum pressure in this type of wing was higher than the maximum pressure in the simple wing. In addition to the higher pressure produced in this type of wing, the flow velocity in the wing with a sinusoidal attack edge is also lower than the simple wing. In addition, it was observed that the absolute pressure is lower in sinusoidal depressions and this pressure difference causes the first point of flow separation along the depressions.

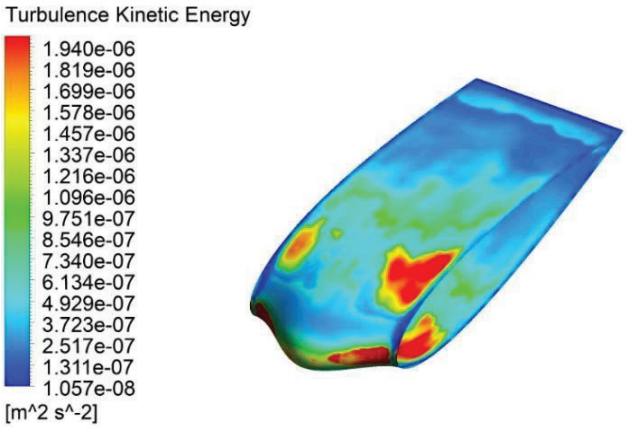


**Figure 8.** Distribution kinetic energy distribution on the wing with a sine attack edge at an angle of attack of 5 ° and a Reynolds number of 60,000.

Figure 8 shows the kinetic energy distribution of turbulence on the wing with a sine strike edge in the Reynolds 60,000. According to this figure, there is a maximum kinetic energy coefficient of turbulence at the volatile edge. This level of energy results in the formation and longer life of a pair of rotating vortices that draw their energy from the shear layer. These pairs of vortices can also act as an overlap layer between the slowly separating layer and the shear layer separated in the flow.

Figure 9 (a), (b) and (c) show the kinetic energy distribution of the turbulence on the wing with a sine wave escape edge in the Reynolds numbers 5000, 15000 and 60,000. The depression of the wing is at its maximum due to the vortex in the area, while the amount of vortices created in other

areas with less geometric changes is not very visible, based on the kinetic energy distribution of the turbulence, moving away from the edge of the attack. First, the kinetic energy of the turbulence increases but then decreases, as shown in Figure 9. As the Reynolds number increases, the kinetic energy of the turbulence on the fin increases sharply. The kinetic energy of the turbulence is slightly diffused at first and is located in the attack edge area and on the sides of the fin, but as the current intensifies, the kinetic energy of the turbulence accumulates in the center of the fin and near the edge of the escape, causing a strong vortex in this area.

Figure 10 (a), (b) and (c) also show the kinetic energy distribution of turbulence on the airfoil surface in Reynolds 5000, 15000 and 60,000, respectively. The fin depression is maximal due to the formation of vortices in this area, while in other areas the amount of kinetic energy of the turbulence is very small, which can be ignored. In addition, according to Figure 10 (a), in Reynolds similar to the kinetic energy of turbulence in this type of wing is reduced compared to the wing with sinusoidal edge and the maximum area is concentrated in the middle of the wing, while this criterion was slightly higher in wings with sinusoidal edge. And its distribution has been wider

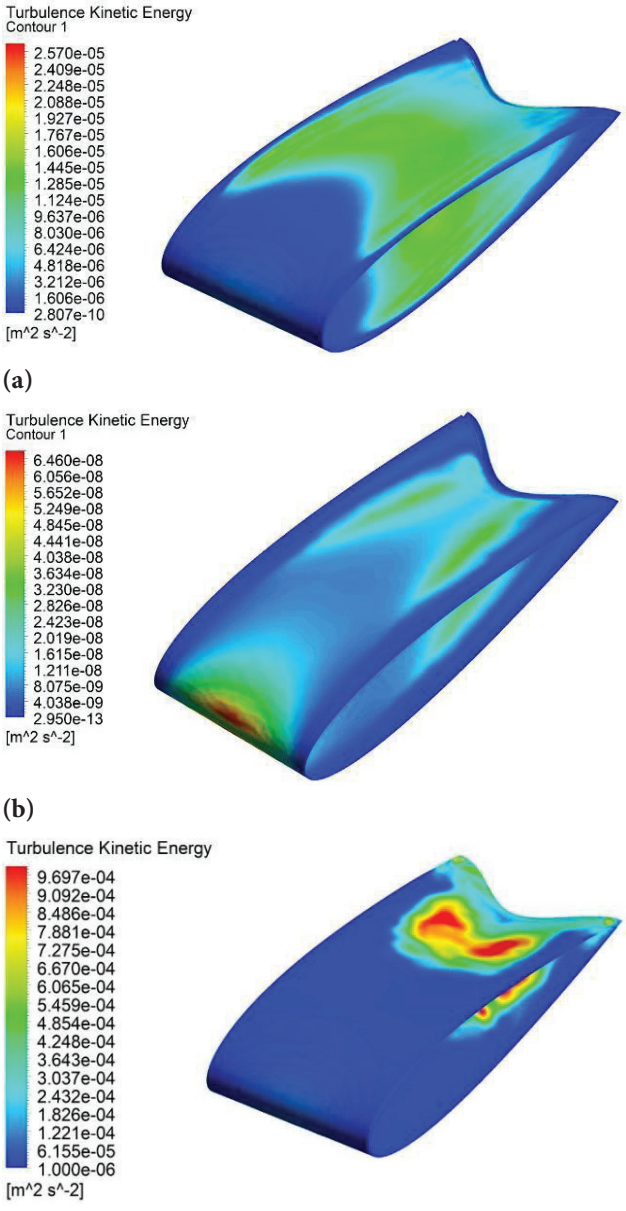


**Figure 9.** Distribution kinetic energy distribution on a wing with a sine wave escape edge in Reynolds (a) 5000 (b) 15000 and (c) 60,000.

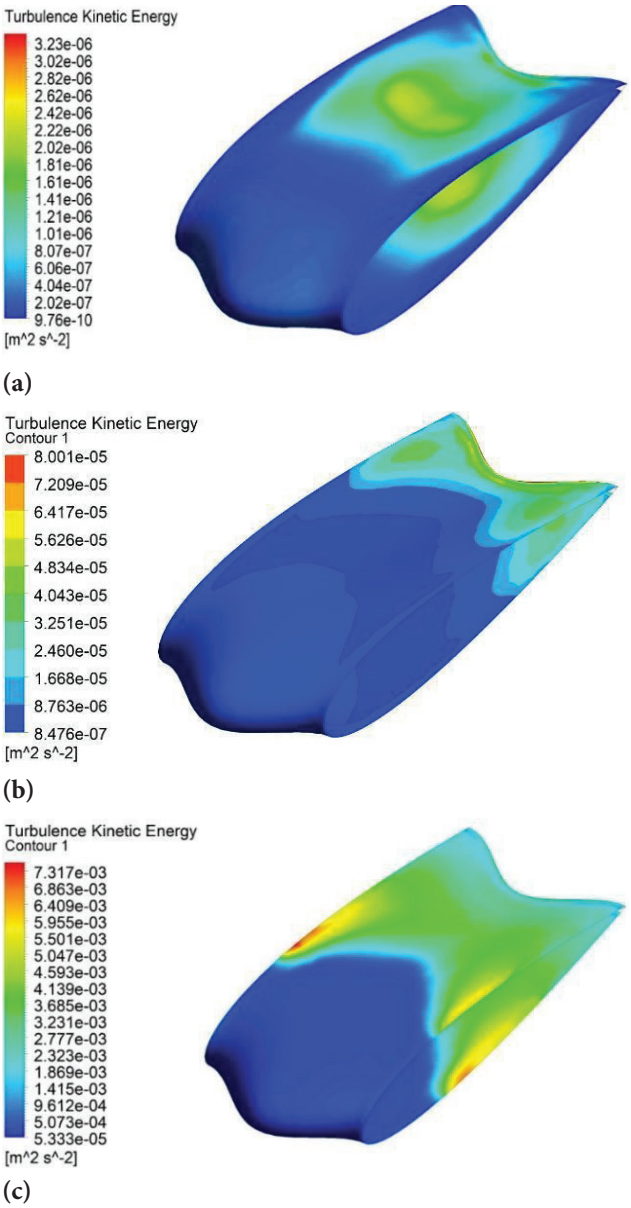


**Figure 10.** Distribution kinetic energy distribution on the wing with volatile edge and sinusoidal attack in Reynolds (a) 5000 (b) 15000 and (c) 60,000.

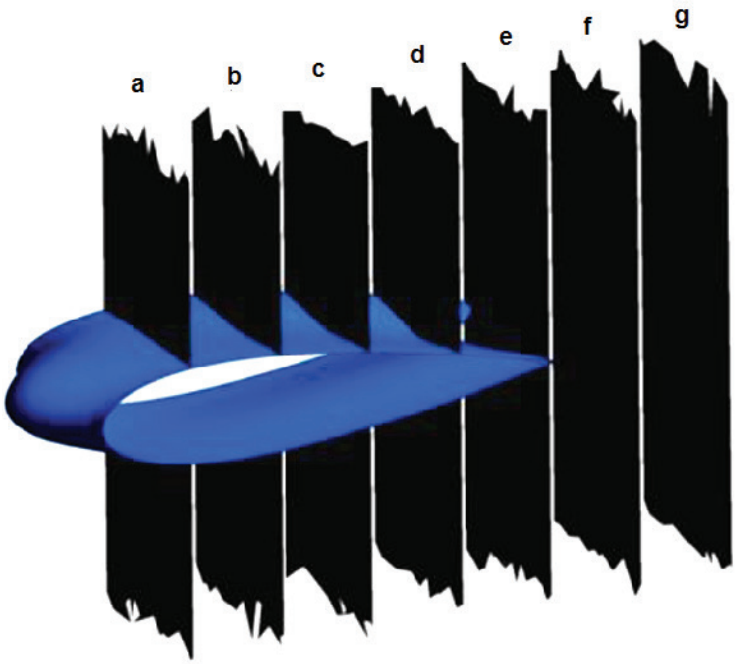


**Figure 11.** Different sections of pages (a), (b), (c), (d), (e), (f) and (g) on the wing with a combined design with a distance of 0.2 and 0.4, respectively. 0.6, 0.8, 0.1, 1.2 and 1.4 chord length from the edge of the attack.

on the wing body. According to Figure 10, it can be seen that the maximum amount of turbulent kinetic energy is transferred from the center of the fin to its sides. The sine at the Reynolds numbers 5000, 15000 and 60,000 is 32 and 8 times higher than its previous Reynolds number, respectively.

Figure 11 shows the different sections for a wing with a composite design. Figure 12 shows the flow lines on each of the above pages. According to this figure, at the beginning of the wing, very small vortices are formed near the surface of the wing, but by moving away from the attacking tip, the size of these vortices has increased sharply. The formation of a pair of primary clockwise and counterclockwise vortices and their overlap and then the formation of secondary vortices will increase the momentum of the current and the flow will stick to the wing surface. It is also observed that at a distance of 0.4 chord length from the edge, the amount of vortices is in its greatest state, and then, as it approaches the attack edge, the location of the vortices is marginalized. Then, in the form of flow lines behind the wing, it is observed that when the current leaves the wing, the location of the vortices is again directed from the margin to the center and the flow is in the form of strong vortices behind the wing.

Figure 13 (A & B) shows the ascending and descending coefficients for simple wing types, with sine attack edge, sine escape edge, and sine escape edge and attack at 5000 Reynolds number and at different attack angles. According to this figure, the coefficient of elevation for a simple wing has been higher than other wings at times, but with increasing angle, the coefficient of elevation decreases and other wings show a higher coefficient of elevation. Based on the obtained results, the wing with sinusoidal evaporation edge has shown a better performance and has a higher coefficient of performance than other sinusoidal wings. Based on these results, in Reynolds number 5000, with increasing the angle of attack, the drag coefficient of different types of wings is always ascending. However, the rate of increase was first increasing and then decreasing. In fact, the simple wing initially had the highest coefficient of elevation, but after the critical angle and separation of the flow, its performance has decreased sharply. But in sinusoidal wings, these changes have been less, in fact, the presence of sinusoidal edges at the point of escape and attack of the wing, has led to reduced flow separation and thus reduced the effects of current on wing performance at critical angles. Figure 14 (A & B) also shows the lifting coefficient diagram of the different wing post coefficients in the Reynolds number 15000, respectively, according to the obtained numerical results. An angle of 22.5 degrees is also observed, and these changes are also observed in the wing with a sinusoidal edging edge, but in the wing with a sinusoidal edging edge, these effects are reduced.

In fact, the results show that in the initial angles of the simple wing has shown better performance than other types of wings; However, with the increase of the angle and reaching the critical angle (about 22.5 degrees) and a significant drop of the lifting coefficient in this type of wing, its performance has sharply decreased. Combined design wings are the best option. Figure 15 (A) shows the

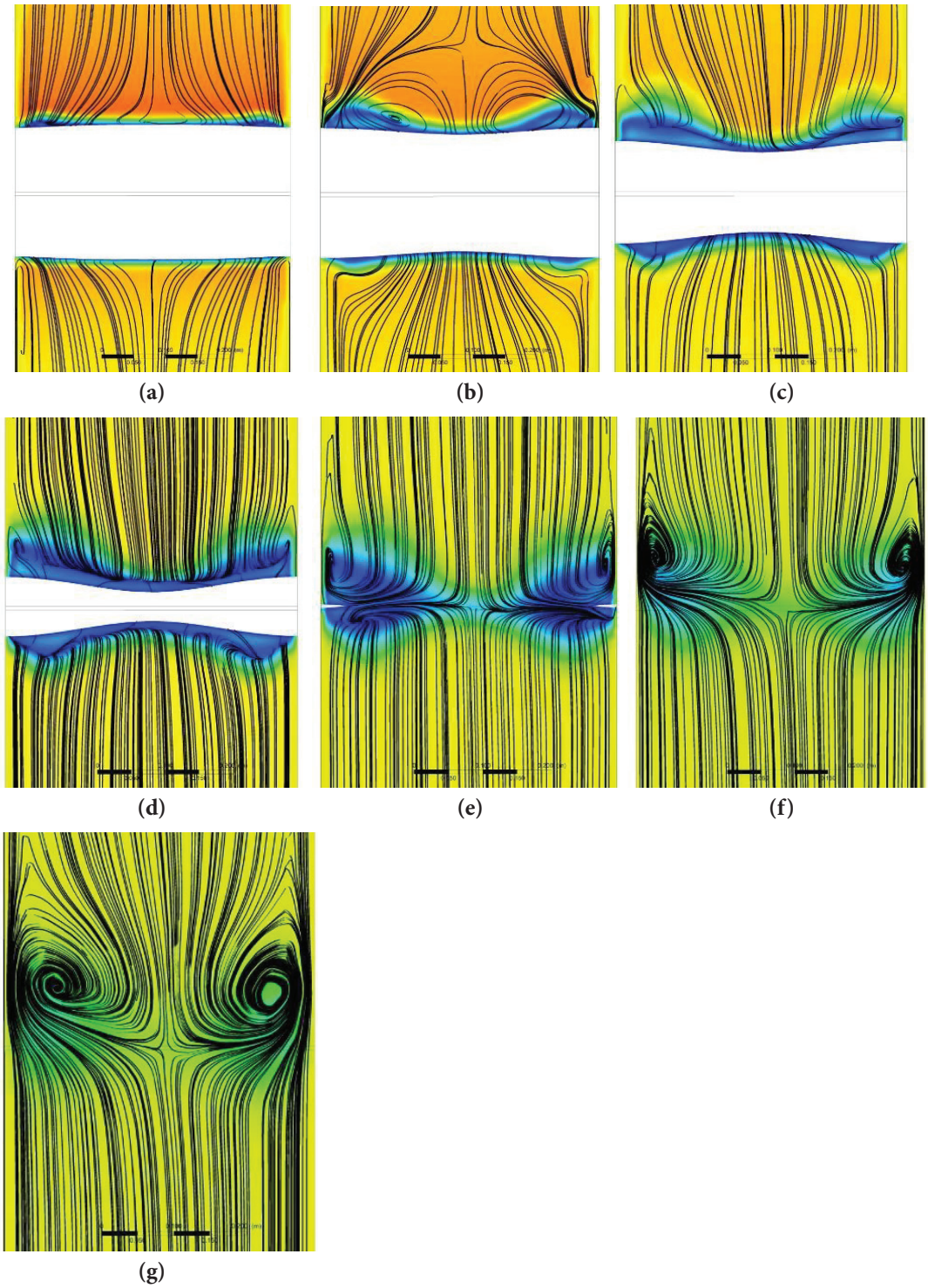


**Figure 12.** Flow lines at 5° angle of attack and Reynolds number 15000 in wing with combined design.

height coefficient of the wing with different airfoils, the largest difference in the coefficient of elevation is related to the angle of 20 degrees. With sinusoidal escape edge and wing with sinusoidal escape and attack edge are 1.1, 0.87, 0.97 and 0.93, respectively. In contrast, the performance of simple fin and fin with sinusoidal escape edge decreases sharply after the phenomenon of exhaustion, while this phenomenon is not observed in the other two fins. At different attack angles. In addition to, the amount of drag coefficient in different angles of attack is seen in Figure 15 (B). Based on the results for the drag coefficient, it is observed that the lowest drag coefficient belongs to the simple wing and the highest to the wing with escape edge and sinusoidal attack at the same time. For example,

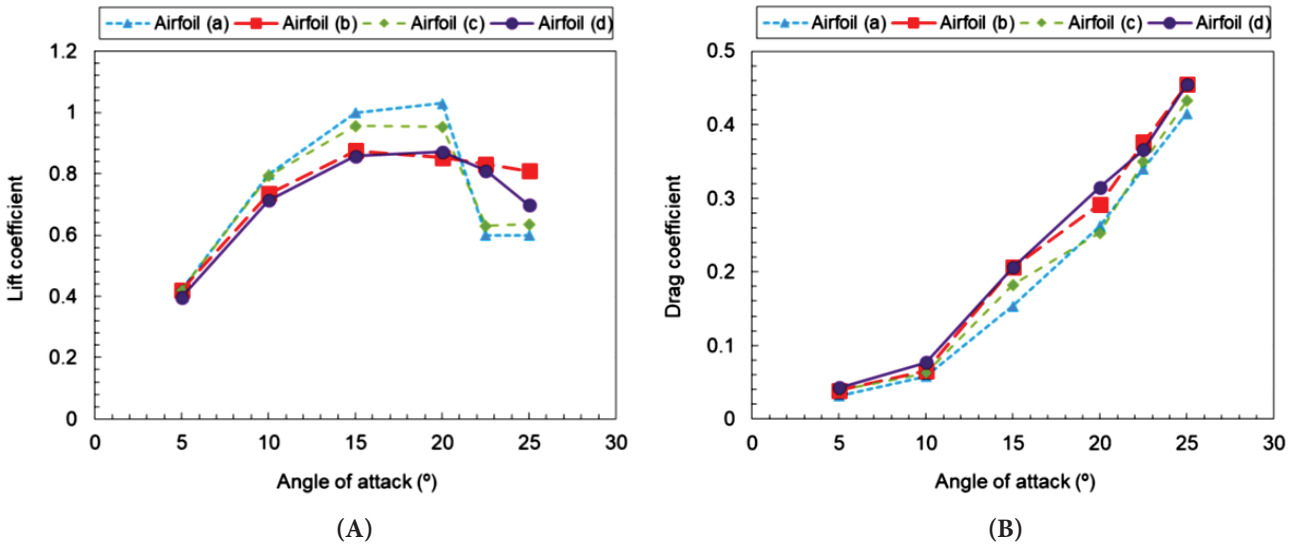


**Figure 13.** (A) The coefficient of elevation (B) The coefficient of drag for different types of wings (a) Simple wings, (b) Wings with sine attack edge, (c) Wings with sine escape edge, (d) Wings with a hybrid design in number Reynolds 5000.

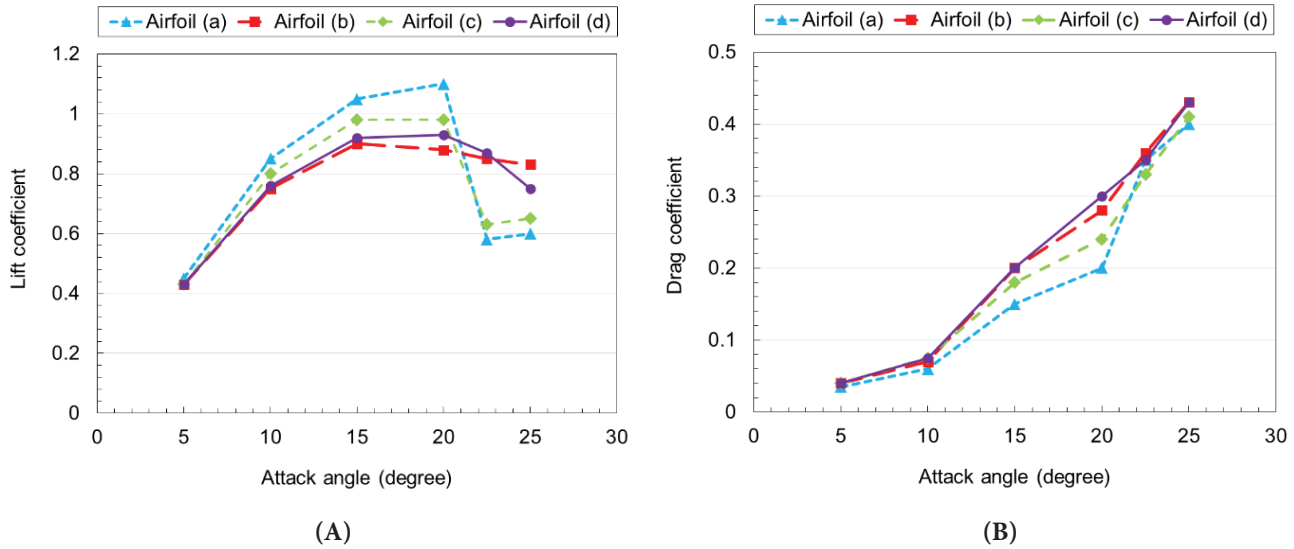


**Figure 14.** (A) Coefficient of elevation (B) Coefficient of drag for wing types (a) Simple wing, (b) Wing with sinusoidal edging edge, (c) Wing with sinusoidal escape edge, (d) Wing with hybrid design in number Reynolds 15,000.

at an angle of attack of 20 degrees, which is on the verge of exhaustion, the drag coefficient for a simple fin, a fin with a sinusoidal attack edge, a fin with a sinusoidal escape edge, and a fin with an escape and attack edge. The sine is 0.20, 0.28, 0.24 and 0.30, respectively. According to the obtained data, it is observed that in sinusoidal wing types, the wing with sinusoidal escape edge has the lowest drag coefficient. In addition, the ascending and descending coefficients of the various types of wings in the Reynolds number 60,000 are shown in Figure 15. According to this figure, with increasing the Reynolds number from 5000 to 60,000, the ascending coefficient increases and the drag coefficient decreases. In addition to, the ratio coefficient and drag coefficient in Reynolds number 60,000 compared to Reynolds number 5000 and 15000 has a significant increase. Based on the numerical results, with increasing Reynolds number, the performance of the wing with a sine attack edge has surpassed the wing with the combined design. In Reynolds numbers less than 60,000, the coefficient of the ball-with-combination design simultaneously after the critical angle is higher than the ball-carrying coefficient with the sine attack edge. It is seen in the Reynolds number 60,000 that this result has changed.

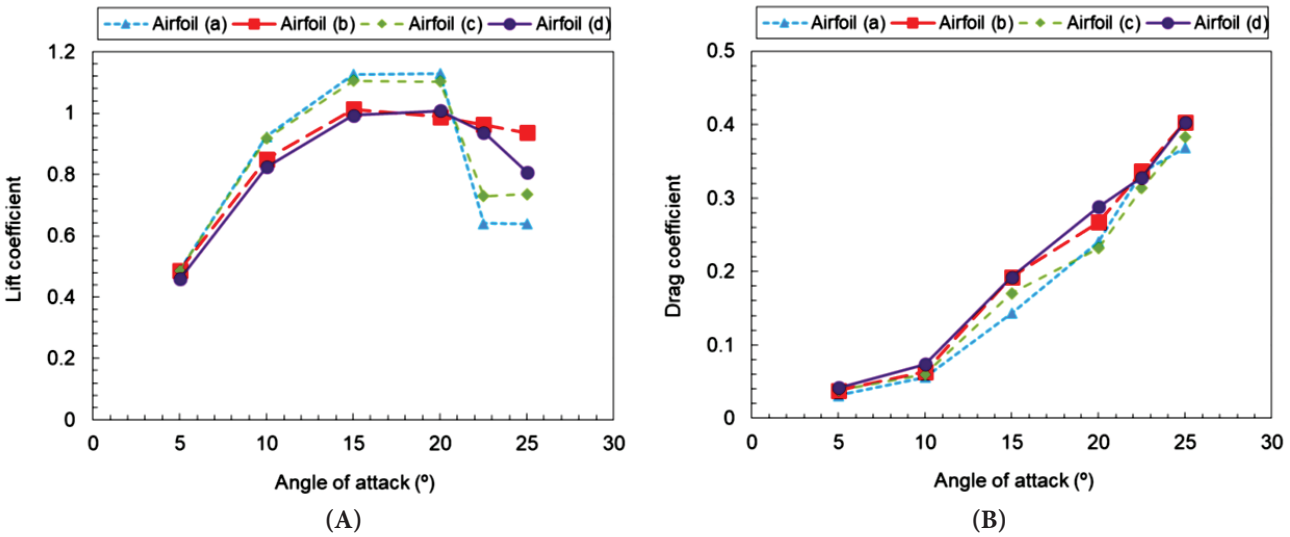


**Figure 15.** (a) The coefficient of elevation b) The coefficient of drag for different types of wings a) Simple wings, b) Wings with sine attack edge, c) Wings with sine escape edge, d) Wings with a compound design in number Reynolds 60,000.

## CONCLUSION

In the present study, a numerical simulation was performed on the wing with different geometries such as simple wing, wing with sinusoidal attack edge, wing with sinusoidal escape edge and wing with combined design, the most important results of which are as follows:

- The maximum amount of pressure around the geometry on the wing with the sine attack edge and the wing with the combined design was higher than the simple wing. In addition to, the speed of flow around this type of wings has been reported to be lower than simple wings.

The kinetic energy of the turbulence on the wing with the sinusoidal escape edge was at its highest, while this criterion was the lowest on the wing with the sinusoidal attack edge.

- The lowest oscillation for the lift coefficient in different types of wings belonged to the hybrid design wing, although this type of wing had the highest drag coefficient. It also delays the fatigue angle and reduces its intensity in reducing the coefficient.
- Among the sinusoidal wings, the lowest drag coefficient belonged to the wing with sinusoidal escape edge.

## AUTHORSHIP CONTRIBUTIONS

Authors equally contributed to this work.

## DATA AVAILABILITY STATEMENT

The authors confirm that the data that supports the findings of this study are available within the article. Raw data that support the finding of this study are available from the corresponding author, upon reasonable request.

## CONFLICT OF INTEREST

The author declared no potential conflicts of interest with respect to the research, authorship, and/or publication of this article.

## ETHICS

There are no ethical issues with the publication of this manuscript.

## REFERENCES

[1] Lang X, Song B, Yang W, Song W. Aerodynamic performance of owl-like airfoil undergoing bio-inspired flapping kinematics. Chin J Aeronaut 2021;34:239−252. [CrossRef]

[2] Abo-Serie E, Oran E, Utcu O. Aerodynamics assessment using CFD for a low drag Shell Eco-Marathon car. J Therm Engineer 2017;3:1527−1536. [CrossRef]

[3] Fish FE, Howle LE, Murray MM. Hydrodynamic flow control in marine mammals. Integr Comp Biol 2008;48:788−800. [CrossRef]

[4] Chen H, Pan C, Wang JJ. Effects of sinusoidal leading edge on delta wing performance and mechanism. Sci China Tech Sci 2013;56:772−779. [CrossRef]

[5] Post ML, Decker R, Sapell AR, Hart JS. Effect of bio-inspired sinusoidal leading-edges on wings. Aerosp Sci Technol 2018;81:128−140. [CrossRef]

[6] Mehraban AA, Djavareshkian MH, Sayegh Y, Forouzi Feshalami B, Azargoon Y, Zaree AH, et al. Effects of smart flap on aerodynamic performance of sinusoidal leading-edge wings at low Reynolds numbers. J Aerosp Engineer 2021;235:439−450. [CrossRef]

[7] Wang T, Feng LH, Li ZY. Effect of leading-edge protuberances on unsteady airfoil performance at low Reynolds number. Exp Fluids 2021;62:217. [CrossRef]
[8] Guo Q, He X, Wang Z, Wang J. Effects of wing flexibility on aerodynamic performance of an aircraft model. Chin J Aeronaut 2021;34:133-142. [CrossRef]
[9] MacPhee DW, Kincaid K, Luhar M. Aerodynamic behavior of curved flexible wings. J Fluids Struct 2022;112:103609. [CrossRef]
[10] Butt U, Hussain S, Schacht S, Ritschel U. Experimental investigations of flow over NACA airfoils 0021 and 4412 of wind turbine blades with and without Tubercles. Wind Engineer 2022;46:89−101. [CrossRef]
[11] Ahmed T, Amin MT, Islam SMR, Ahmed S. Computational study of flow around a NACA 0012 wing flapped at different flap angles with varying Mach numbers. Glob J Res Engineer 2014;13:4−16.
[12] Zhang Y, Huang Y, Wang F, Tan Z. Numerical simulation of the airfoil flowfields at angles of attack from 0° and 180°. Asia-Pacific Power and Energy Engineering Conference; 2010. [CrossRef]
[13] Windi IS, Faris MA, Kareem H. Experimental and theoretical investigation for the improvement of the aerodynamic characteristic of NACA 0012 airfoil. Int J Min Metall Mech Engineer 2014;2:11−15.
[14] Laouira H, Mebarek-Oudina F, Hussein AK, Kolsi L, Merah A, Younis O. Heat transfer inside a horizontal channel with an open trapezoidal enclosure subjected to a heat source of different lengths. Heat Transfer-Asian Res 2019;49:406−423. [CrossRef]
[15] Hassan M, Mebarek-Oudina F, Faisal A, Ghafar A, Ismail AI. Thermal energy and mass transport of shear thinning fluid under effects of low to high shear rate viscosity. Int J Thermofluids 2022;15:100176. [CrossRef]
[16] Miklosovic DS, Murray MM. Experimental evaluation of sinusoidal leading edges. J AIRCRAFT 2007;44:1404. [CrossRef]
[17] Pendar MR, Esmaeilifar E, Roohi E. LES study of unsteady cavitation characteristics of a 3-D hydrofoil with wavy leading edge. Int J Multiphase Flow 2020;132:103415. [CrossRef]
[18] Chung TJ. Computational Fluid Dynamics. Cambridge: Cambridge University Press; 2002.
[19] Lei Z. Effect of RANS turbulence models on computation of vortical flow over wing-body configuration. Trans Jpn Soc Aeronaut Space Sci 2005;48:152−160. [CrossRef]
[20] Hansen KL, Rostamzadeh N, Kelso RM, Dally BB. Evolution of the streamwise vortices generated between leading edge tubercles. J Fluid Mech 2016;788:730−766. [CrossRef]